

3-D MRI assessment of regional left ventricular systolic wall stress in patients with reperfused MI

Stephane Delépine,¹ Alain P. Furber,¹ Farzin Beygui,¹ Fabrice Prunier,¹ Philippe Balzer,² Jean-Jacques Le Jeune,² and Philippe Geslin¹

Departments of ¹Cardiology and ²Biophysics, University Hospital of Angers, 49033 Angers Cedex 01, France

Submitted 8 February 2002; accepted in final form 20 September 2002

Delépine, Stephane, Alain P. Furber, Farzin Beygui, Fabrice Prunier, Philippe Balzer, Jean-Jacques Le Jeune, and Philippe Geslin. 3-D MRI assessment of regional left ventricular systolic wall stress in patients with reperfused MI. *Am J Physiol Heart Circ Physiol* 284: H1190–H1197, 2003. First published October 10, 2002; 10.1152/ajpheart.00106.2002.—The goal of this study was to assess the regional variations of end-systolic wall stress in patients with reperfused Q wave acute myocardial infarction (AMI), with the use of a three-dimensional (3-D) approach. Fifteen normal volunteers and fifty patients with reperfused AMI underwent cardiac MRI that used a short-axis fast-gradient-echo sequence. The end-systolic wall stress was calculated with the use of the Grossman formula with the radius and the wall thickness defined with a 3-D approach using the tridimensional curvature. The mean wall stress was significantly increased at each level of the short-axis plane only in patients with anterior AMI. When calculated at a regional level in patients with anterior AMI, wall stress significantly increased in anterior sector as well as normal sector. In patients with inferior AMI, wall stress significantly increased only in inferior and lateral sectors. In conclusion, the quantification of regional wall stress by cardiac MRI is better with the 3D approach than other methods for precise evaluation in patients with AMI. Despite early reperfusion, the wall stress remained high in patients with anterior AMI.

left ventricular remodeling; left ventricular function; cardiac imaging

LEFT VENTRICULAR REMODELING, a factor of poor prognosis (29), begins on formation of the infarction (11) and can continue after the cicatrization phase (13). The modifications of ventricular geometry concern the infarcted zone, which is subjected to a phenomenon of expansion associated with wall thinning, and the healthy zone, which will hypertrophy and then dilate (17). Remodeling intensity is a function of neurohormonal factors linked with activation of the renin-angiotensin system (19) and the sympathetic nervous system (6), together with mechanical factors, depending on the size and the localization of the infarction (28) and on the afterload evaluated by the end-systolic wall stress (20).

The end-systolic wall stress is the product of the systolic pressure of the left ventricle (or its estimation)

and a geometric factor dependent on the shape of the left ventricle (5). The geometry of the left ventricle in infarction is complicated, and only a tridimensional approach, excluding the use of a geometric model, is valid in the presence of ventricular deformations, which can occur after myocardial infarction. Because of good spatial resolution and an absence of a geometric hypothesis, the MRI allows precise definition of the epicardial and endocardial borders of the left ventricle (1, 8).

Several mathematical models have been used to calculate the wall stress. Some (10) depend on the shape of the left ventricle and are only valid in the presence of a ventricle of spheroid or ellipsoid shape and only allow calculation of the global wall stress. Others are applicable whatever the shape of the left ventricle (12). These different methods remain valid for the equatorial region of the latter; however, they lead to systematic overestimation of the thickness of the left ventricular wall and underestimation of the radius of curvature (4), as we have reported in the normal subject (2). In myocardial infarction, Pouleur et al. (21), in utilizing the Janz formula, found that the precision of the method decreases in the apical region of the left ventricle, where there are considerable variations in the radius of curvature. Our tridimensional approach allows the best possible assessment of the regional variations of the wall thickness and the radius of curvature in the three planes of space (2).

The aim of this study was to assess the regional variations of the end-systolic wall stress provided by breath-hold fast-gradient echo MRI, in patients with Q wave acute myocardial infarction (AMI) undergoing successful reperfusion, with the use of a tridimensional approach where the wall curvature is taken into account.

METHODS

Study Population

The study included patients with Q wave AMI undergoing a successful reperfusion. The inclusion criteria were 1) typical angina pain lasting >30 min, 2) ST segment elevation of at least 2 mm in two or more contiguous leads, and 3) a

Address for reprint requests and other correspondence: A. Furber, Dept. of Cardiology, the Univ. Hospital of Angers, 4 rue Larrey, 49033 Angers Cedex 01, France (E-mail: alfurber@chu-angers.fr).

The costs of publication of this article were defrayed in part by the payment of page charges. The article must therefore be hereby marked "advertisement" in accordance with 18 U.S.C. Section 1734 solely to indicate this fact.

greater than twofold increase in serum MB creatine kinase levels. The exclusion criteria were a history of myocardial infarction and the contraindication to MRI exam. Patients were ineligible for the study if they had a pacemaker, a cardioverter-defibrillator, intracranial clips, intra-auricular or intraocular implants, a history of metal fragments in the eyes, claustrophobia, and a heart rhythm other than the normal sinus. The study protocol was approved by the ethics committee of the University Hospital of Angers, and informed consent was obtained.

Fifty patients were consecutively included in the study. The average age was 56 ± 14 yr (range 27–81 yr). The main characteristics of this population are summarized in Table 1. The infarct-related coronary reperfusion has been performed by direct (43 patients) or rescue (2 patients) coronary angioplasty, by intravenous thrombolysis (2 patients), and spontaneously (aspirin-heparin; 3 patients). The infarct-related coronary reperfusion has been performed within 6 h after chest pain began in 31 patients, within 12 h in 11 patients, and within 48 h in 8 patients. Reperfusion was performed successfully in all patients (Thrombolysis in Myocardial Infarction grade 3 flow and absence of residual stenosis). The AMI localization was anterior in 28 patients, inferior in 20 patients, and lateral in 2 patients. These two patients with lateral infarct were not considered for statistical analysis. The infarct-related arteries in anterior infarct were left anterior descending coronary artery, in inferior infarct were right coronary artery, and in lateral infarct were circumflex. β -Blockers were administered in 86% of the patients. Angiotensin-converting enzyme inhibitors were administered in 76% of the patients, in 90% of patients with anterior infarct, and in 60% of patients with inferior infarct. The average time between AMI and MRI was 11 ± 10 days.

Normal Population

The normal study population consisted of 15 healthy volunteers (9 men and 6 women) with a mean age of 28 ± 7 yr, and with no history or physical finding of cardiac or pulmo-

nary disease. The average systolic and diastolic arterial pressures were 127 ± 6 and 77 ± 7 mmHg, respectively.

Imaging Technique

All normal subjects and patients were studied with a 1.5-T imager (Signa Horizon 5.7, GE Medical Systems; Milwaukee, WI). The subjects were placed in supine position with a phased-array coil (torso coil). A fast-gradient echo segmented k -space sequence with radio frequency phase spoiling was used with ECG gating. Scout transversal and sagittal views ensured correct determination of the short-axis plane of the left ventricle. Each section was then acquired in a single breath hold (20–25 s) with 12 to 26 temporal phases per heartbeat using view sharing and uniform repetition time radio frequency excitation. The interleaved images were obtained in 8–12 planes from the apex to the base with the following parameters: 10-mm section thickness, no gap between sections, 320-mm field of view, partial echo, 2.7-ms echo time, 10.2-ms repetition time, 15.6-kHz receiver bandwidth, 30° flip angle, 8 views per segment, 256×128 mm matrix, 1.25×1.25 mm pixel size, and 1 excitation.

Image Analysis

For analysis and computation, the MR images were transferred to a multimodality station (model HP 715–50, Hewlett-Packard; Palo Alto, CA) with UNIX. The endocardial and epicardial borders of the left ventricle were drawn with an automatic segmentation method previously validated in animals and patients (1, 8).

Regional End-Systolic Wall Stress

The multisection images at the end-diastolic and end-systolic phases were determined by locating the largest and the smallest areas of the left ventricular cavity on a midventricular short-axis plane. On all sections, the centroid of the left ventricle was located as the mass center of the median line between the endocardial and epicardial borders. Each short-axis section was centered on the mean position of the ventricular centroid during the cardiac cycle. The wall stress was studied on a set of five contiguous short-axis planes (Fig. 1). For all volunteers and patients, the set encompassed sections with closed and clearly defined endocardial and epicardial borders.

The calculation of the wall curvature relies on a polar transformation of the image. This process has been widely used for segmentation algorithms (7) and allows a radial study of the left ventricle. With a centerline approach (27), the wall curvature from the base to the apex is assessed on 128 radii, and the left ventricular radius and wall thickness are deduced from the geometry of the ventricle on two consecutive short-axis sections (2, 4). The main steps of the method have been previously described (2). Briefly, for the wall stress assessment, the apical planes with no ventricular cavity and the valvular planes with an open chamber were excluded from the analysis. A set of five contiguous short-axis planes was studied. The set was centered on midventricular plane, which was defined as level of the papillary muscle insertions. At left, the short-axis planes were located at 10 and 20 mm toward the apex, and at right toward the base. From this set of five contiguous short-axis planes, four thick slices were interposed to calculate the three-dimensional (3-D) thickness and 3-D radius of curvature. The end-systolic wall stress was subsequently measured on four contiguous levels and was averaged in the anterior, lateral, inferior, and septal sectors (Fig. 2).

Table 1. Clinical characteristics and hemodynamic data of AMI study population

Characteristics	Values
Age, yr	55.6 ± 14
Men ($n = 43$)	86*
Hypertension ($n = 15$)	30*
Hypertension in patients with inferior AMI ($n = 5$)	25*
Hypertension in patients with anterior AMI ($n = 9$)	32*
Diabetes mellitus ($n = 3$)	6*
Active smoker ($n = 35$)	70*
Hypercholesterolemia ($n = 22$)	44*
Systolic arterial blood pressure, mmHg	116 ± 19
Diastolic arterial blood pressure, mmHg	73 ± 12
Time to reperfusion, h	8.5 ± 10.1
Infarct-related coronary artery, LAD/CX/RCA	28/2/20
Peak CPK, CPK-MB	2,684 (406)
Angiographic parameters	
End-diastolic volume, ml/m ²	136 ± 49
End-systolic volume, ml/m ²	78 ± 48
Ejection fraction, %	51 ± 10

Values are means \pm SD; n , no. of patients. AMI, acute myocardial infarction; LAD, left anterior descending coronary artery; CX, circumflex; RCA, right coronary artery; CPK, creatine phosphokinase. *Numbers refer to percentages.

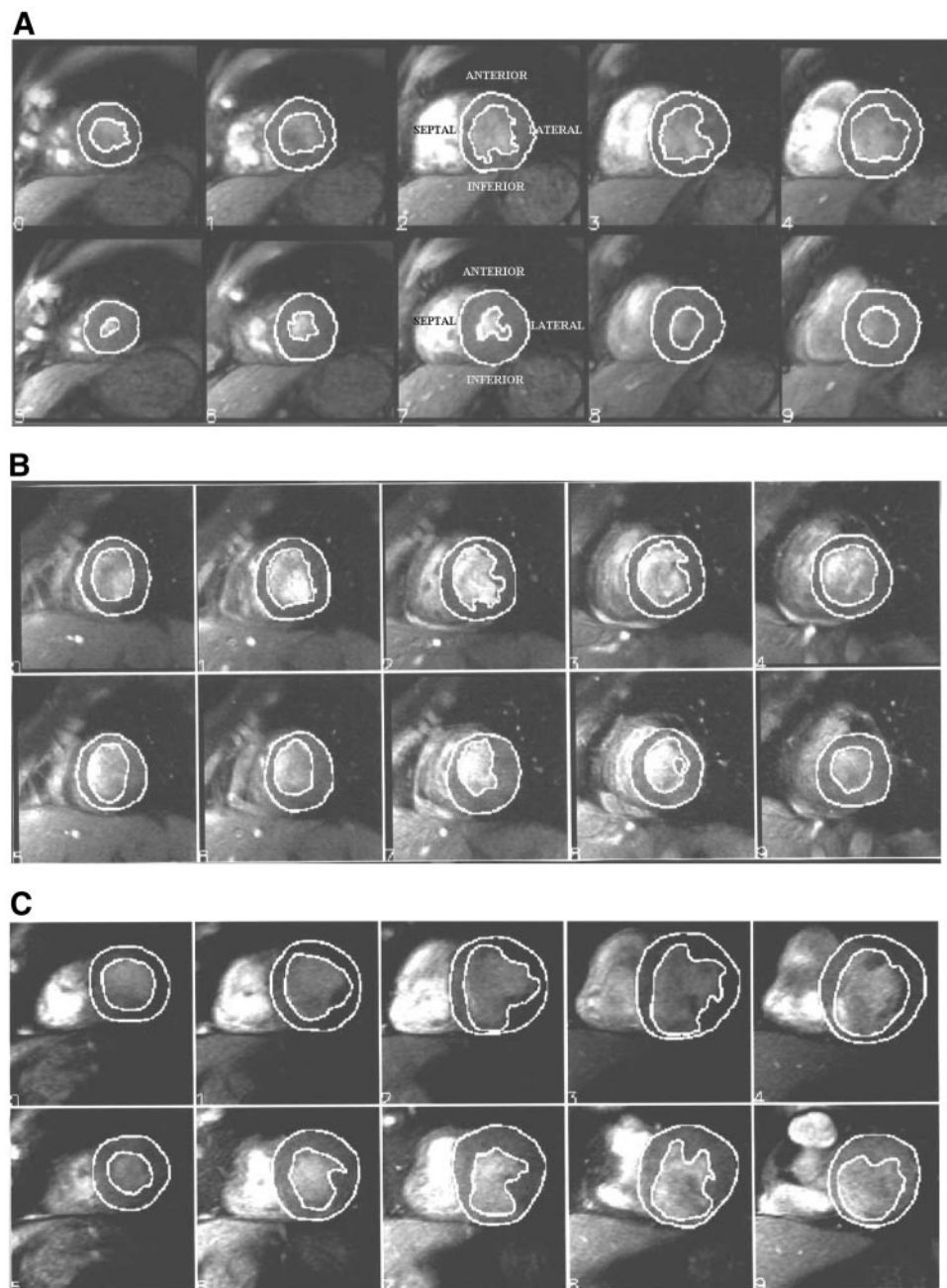


Fig. 1. A set of five adjacent short-axis MRIs of the left ventricle at the end-diastolic (*top*) and end-systolic (*bottom*) phases in normal subjects (*A*), and in patients with anterior (*B*) and inferior (*C*) infarction.

Computation of Regional End-Systolic Wall Stress

End-systolic wall stress was calculated using the Grossman formula

$$WS = 0.133 \times SP \times \frac{R}{2T \times \left(1 + \frac{T}{2R}\right)}$$

where SP is the peak systolic ventricular blood pressure (in mmHg), and 0.133 is a conversion factor to express the final results in 10^3 N/m^2 .

Inner radius R and wall thickness T were calculated with a two-dimensional approach (ESR and EST, respectively) as reported by Grossman (10) and with the radius and wall thickness (3DES and 3DEST, respectively) defined with our 3-D approach using the tridimensional curvature (3DWS).

End-systolic wall stress was also calculated by using the Janz method (12)

$$AWS = 0.133 \times SP \times \frac{A_w}{A_c}$$

This approach relies on the measurement of the areas A_c and A_w of the blood pool and the ventricular wall, respectively.

In this study, the peak systolic ventricular blood pressure was assessed by the peak systolic noninvasive blood pressure (22) with five measurements recorded (using the Maglife system) and averaged at the time of the MRI examination.

Global Left Ventricular Function and Wall Thickening

The following parameters were calculated. First, end-diastolic volume (EDV), end-systolic volume (ESV), and ejection

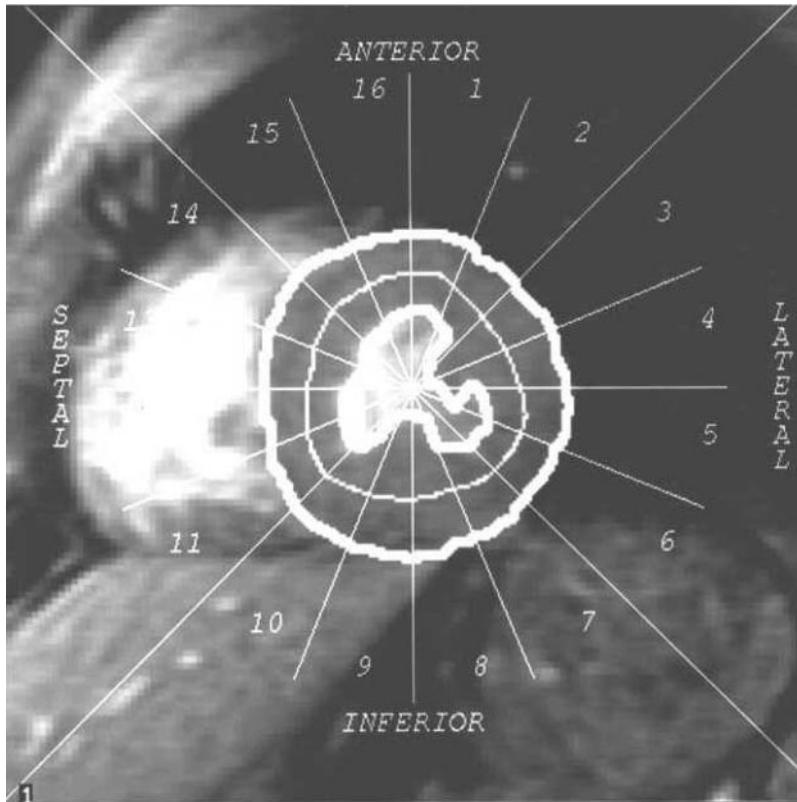


Fig. 2. Sectorial analysis of the left ventricular wall at end systole.

fraction (EF) of the left ventricle determined by $EF (\%) = (EDV - ESV)/EDV$. Second, the mass of the left ventricle (in grams) given by

$$M = \sum_{i \leq n} A_{w_i} \cdot t \cdot \rho$$

where t is the thickness of the n short-axis slices, A_{w_i} is the area of the ventricular wall on the slice i , and ρ is the density of myocardial tissue equal to 1.05 g/cm^3 .

Third, tridimensional wall thickening is $3DWT (\%) = (3DEST - 3DEDT)/3DEDT$, where $3DEDT$ is the wall thickness at the end diastole, according to spatial curvature.

Statistical Analysis

Data are expressed as means \pm SD. The comparison of bidimensional and tridimensional evaluation of the regional wall stress, wall thickening, and radius of curvature were made by ANOVA. Scheffé's subtesting was used to test the significance of difference between the method. The gradient of the wall stress from the apex to the base was assessed for each formulation by ANOVA with Scheffé's subtesting for comparison between the adjacent levels. Statistical significance for comparison of 3-D MRI assessment of regional left ventricular systolic wall stress in patients with reperfused myocardial infarction (WS), wall stress assessment from measurements of the areas (AWS), 3DWS, EST, 3DEST, ESR, 3DESR, and 3DWT between the controls and the patients with anterior or inferior myocardial infarction was determined using the nonpaired two-tailed Student's t -test. Linear regression analysis was used to define the relationship between the different formulations of the end-systolic wall stress and wall thickening. A P value of ≤ 0.05 was considered statistically significant.

RESULTS

Global Left Ventricular Function

The values of mass, volume, and EF of the left ventricle in normal subjects and patients with anterior or inferior myocardial infarction are given in the Table 2. The end-systolic wall stress was significantly increased only in patients with anterior myocardial infarction, whatever the method to calculate the wall stress. 3DWS was significantly higher than WS and AWS in normal subjects and in patients with anterior or inferior infarction. There was a significant correlation between 3DWS and EF ($r = -0.71$; $P < 0.05$), EDV ($r = 0.57$; $P < 0.05$), and end-systolic volume ($r = 0.74$; $P < 0.05$).

3DWS was significantly lower in patients imaged early. 3DWS, ESV index, and EF were, respectively, $5.6 \times 10^3 \text{ N/m}^2$, 19.9 ml/m^2 , and 53%, in patients imaged on days 1-5, and $8.4 \times 10^3 \text{ N/m}^2$, 30.5 ml/m^2 , and 40% in patients imaged on days 6-21.

Regional Left Ventricular Analysis

Variation of end-systolic wall stress from apex to base. In patients with anterior AMI, WS, AWS, and 3DWS were significantly increased compared with normal values without any significant variation from the apex to the base (see Fig. 3).

In patients with inferior AMI, WS, AWS, and 3DWS were similar to normal values. A gradient from the

Table 2. Global left ventricular function

	Normal	Anterior Infarction	<i>P</i> /Normal Values	Inferior Infarction	<i>P</i> /Normal Values
Mass, g	120 ± 31	140 ± 37	NS	146 ± 41	NS
Mass index, g/m ²	64 ± 13	76 ± 16	0.025	79 ± 15	0.0057
End-diastolic volume, ml	74 ± 16	92 ± 32	0.049	79 ± 17	NS
End-diastolic volume index, ml/m ²	40 ± 6	50 ± 17	0.034	42 ± 9	NS
End-systolic volume, ml	29 ± 10	61 ± 30	<0.001	35 ± 11	NS
End-systolic volume index, ml/m ²	16 ± 5	33 ± 17	<0.001	19 ± 7	NS
Ejection fraction, %	61 ± 8	37 ± 18	<0.001	55 ± 12	NS
Systolic arterial blood pressure, mmHg	127 ± 6	112 ± 18	0.02	123 ± 19	NS
Wall stress WS (103 N/m ²)	5.3 ± 1.9	9.9 ± 5.0	0.0017	5.0 ± 1.8	NS
Wall stress AWS (103 N/m ²)	5.3 ± 2.0	9.6 ± 4.9	0.0024	4.7 ± 1.7	NS
Wall stress 3DWS (103 N/m ²)	8.5 ± 2.9*	14.3 ± 6.2*	0.0014	10.2 ± 4.1*	NS

Values are means ± SD. NS, not significant; WS, wall stress assessment in the short-axis (Grossman method); AWS, wall stress assessment from measurements of the areas (Janz method); 3DWS, wall stress assessment according to tridimensional approach. **P* < 0.05: 3DWS vs. WS and AWS.

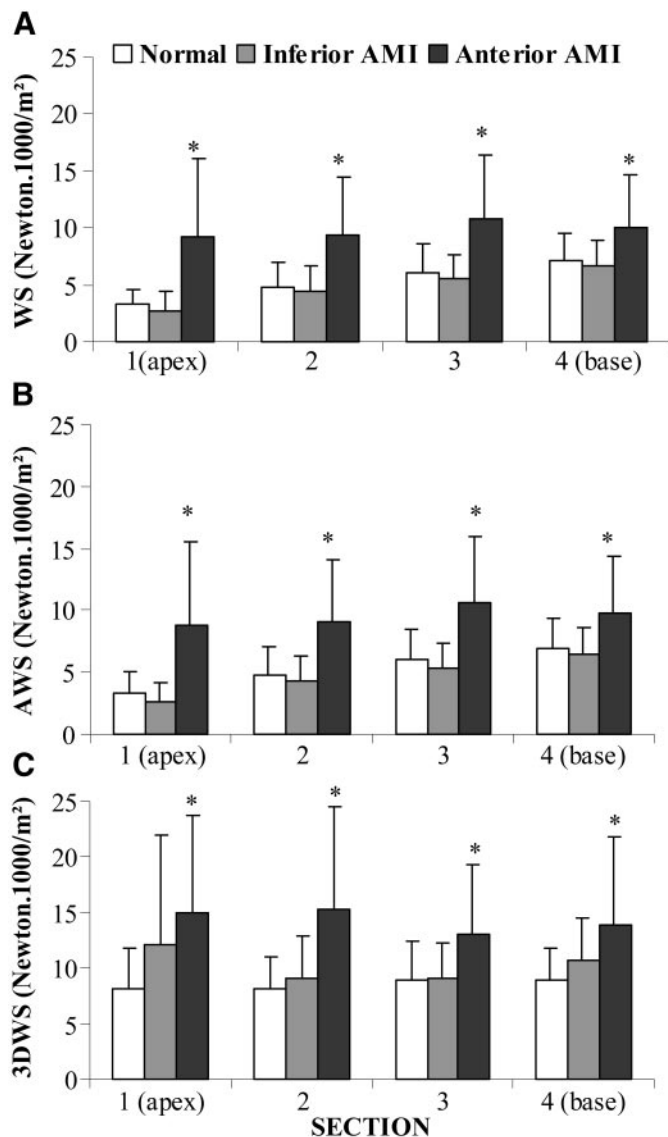


Fig. 3. Variation of the end-systolic wall stress (WS; A), WS assessment from measurements of the areas (AWS; B), and a three-dimensional approach tridimensional curvature (3DWS; C) from the apex to the base of the left ventricle in normal subjects and in patients with anterior and inferior infarction. Values are means ± SD. *Significant difference between patients with anterior or inferior infarction vs. normal subjects. AMI, acute myocardial infarction.

apex to the base was only observed with WS and AWS (ANOVA, *P* < 0.0001).

3DWS was higher than WS and AWS in normal subjects (*P* < 0.01) and in patients with anterior (*P* < 0.05, except level 3) or inferior (*P* < 0.0001) infarction for each level.

Variation of end-systolic wall stress according to sector. In patients with anterior AMI, the wall stress of the anterior sector was significantly higher than the others sectors, whatever method was used (see Fig. 4). Compared with normal values, 3DWS was significantly increased in all sectors, and WS and AWS in anterior, lateral, and inferior sectors.

In patients with inferior AMI, the wall stress of the inferior sector compared with others sectors was significantly higher for WS and AWS but not significant for 3DWS (ANOVA, *P* = 0.08). Compared with normal values, 3DWS was significantly increased in inferior and lateral sectors, without any significant variation for WS and AWS.

3DWS was higher than WS and AWS in normal subjects (*P* < 0.05) and in patients with anterior (*P* < 0.01) or inferior (*P* < 0.0001) infarction for each sector.

The regional wall stresses were not influenced by the presence of hypertension, β-blocker, or angiotensin-converting enzyme inhibitor therapy.

Variation of sectorial analysis of end-systolic wall stress from apex to base. In patients with anterior AMI, WS, AWS, and 3DWS of anterior sector and for each level in the short-axis plane (except level 4 for 3DWS) were significantly increased compared with healthy sectors. In all methods, compared with normal subjects, anterior and lateral sectors were increased (*P* < 0.05) for each plane, whereas inferior and septal sectors were significantly increased only in apical plane.

In patients with inferior AMI, WS, AWS, and 3DWS of inferior sector and for each level (except level 1) in the short-axis plane were significantly increased compared with healthy sectors. Compared with normal subjects, only 3DWS of lateral and inferior sectors for basal plane were significantly increased.

End-diastolic wall thickness. In patients with anterior AMI, compared with normal values, and whatever

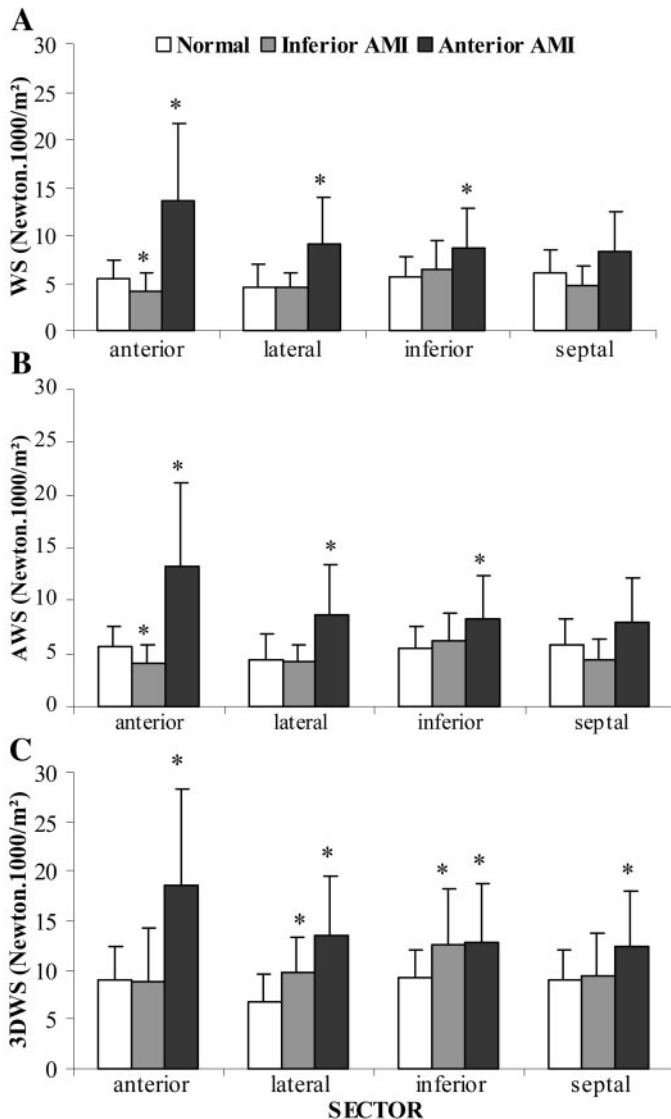


Fig. 4. Variation of end-systolic WS (A), AWS (B), and 3DWS (C) according to sector of the left ventricle in normal subjects and in patients with anterior and inferior infarction. Values are means \pm SD. *Significant difference between patients with anterior or inferior infarction vs. normal subjects.

method was used, the anterior and lateral sectors were similar with hypertrophy in other sectors (see Fig. 5A).

In patients with inferior AMI, the inferior wall thickness was similar compared with normal values with significant hypertrophy in opposite sectors, whatever method was used.

End-systolic wall thickness and radius of curvature. In patients with anterior AMI, compared with normal values and whatever method was used, the anterior and lateral sectors were significantly thinner without hyperkinesie in other sectors, and the curvature radius was significantly increased in all sectors.

In patients with inferior AMI, the inferior wall thickness was similar to compared normal values with compensatory significant hyperkinesie in opposite sectors, whatever method was used. ESR was not different

from normal values; on the other hand, 3DESR was significantly increased in all sectors.

Wall thickening. In patients with anterior AMI, 3DWT was significantly decreased in all sectors, except septal sector, compared with normal values (Fig. 5B).

In patients with inferior AMI, 3DWT in inferior (not significant) and lateral (significant) sectors were decreased compared with normal values. The 3DWT of septal sector was increased in favor of possible compensatory hyperkinesie.

DISCUSSION

Various experimental studies (14, 16, 23, 25, 30) of myocardial infarction have confirmed the importance of a regional analysis of the wall stress and the need for development of a suitable method of measurement. The resolution and contrast of MR images allow local measurements of wall stress without any geometric assumptions. Pouleur et al. (21) reported an increase of the global end-systolic wall stress in patients with coronary artery diseases; however, few studies have described regional variations of the wall stress in the acute phase of infarction and none in the reperfused infarctions.

Our study shows, in anterior infarction, a diffuse increase of the sectorial wall stress predominant at the level of the infarcted zone. In inferior infarction, only an increase localized at the infarcted zone was observed. These results are in agreement with the works

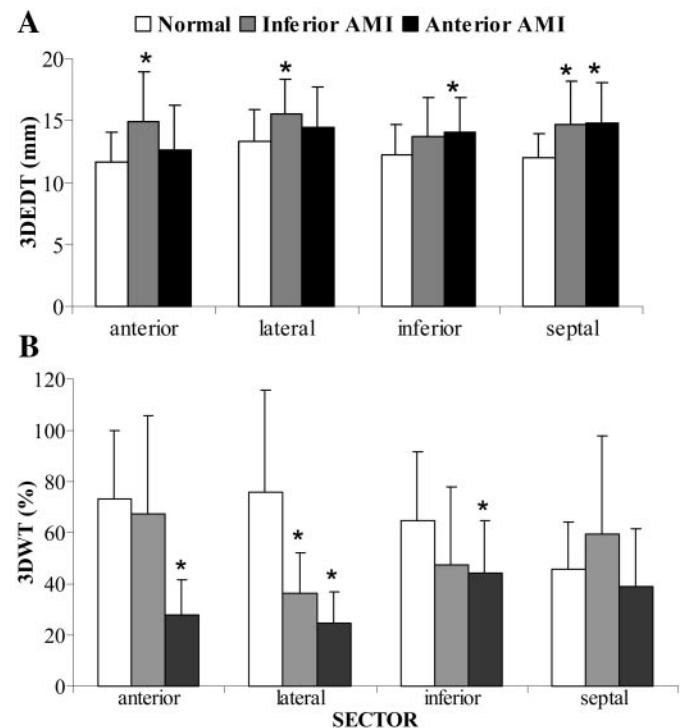


Fig. 5. Variation of end-diastolic wall thickness (EDT; A) and wall thickening (WT; B) according to sector of the left ventricle in normal subjects and in patients with anterior and inferior infarction. 3-D, three-dimensional. Values are means \pm SD. *Significant difference between patients with anterior or inferior infarction vs. normal subjects.

of Ginzton et al. (9) in echocardiography who reported, in anterior nonreperfused infarction, a diffuse increase of the wall stress, whereas this increase remained localized in the inferior region in the nonreperfused inferior infarction. Solomon et al. (26) reported with echocardiography in the nonreperfused anterior infarction an increase of the end-systolic wall stress in the apical region compared with normal subjects and patients with an inferior infarction. On the other hand, Pouleur et al. (20), with angiography and in the presence of former nonreperfused infarctions, observed increased wall stress in ischemic and infarcted zones without abnormality of the healthy zone.

To our knowledge, we are the first to describe the regional variations of wall stress of the anterior, lateral, and inferior walls and the interventricular septum after an acute reperfused infarction.

In patients with anterior infarction, WS, AWS, and 3DWS are increased in all sectors of the most apical sections and only in the infarcted sectors of the most basal sections. This could be explained by a modification of the ventricular geometry of the apical region, which assumes a more spherical shape. This hypothesis seems to be confirmed by Mitchell et al. (18), who used angiography. They reported geometrical modifications in the apical region of the left ventricle three weeks after a nonreperfused anterior infarction, which implies that analysis of the regional curvature constitutes a major determinant of the wall stress.

In patients with inferior infarction, WS, AWS, and 3DWS are normal compared with the healthy subjects when values are averaged for each section. Conversely, at the sectorial level, only 3DWS increases significantly in the infarcted territory compared with the healthy subjects. Compared with the healthy sectors, WS, AWS, and 3DWS increase in the infarcted territory. However, 3DWS was not significantly increased due to a wide standard deviation.

In the normal subject, we showed the importance of calculating the radius of curvature with a tridimensional approach, evidencing the disappearance of the apex-base gradient of the 3DWS regional stress, present with WS and AWS (2). This regional sectorial analysis with a tridimensional approach is, therefore, more appropriate and even useful for a precise evaluation of the left ventricular wall stress with only small regional wall abnormalities. The advantage of the tridimensional approach is avoidance of the erroneous estimation of the radius of curvature and the wall thickness. In fact, with a planar short-axis analysis, the section toward the apex of the left ventricle is no longer perpendicular to the wall, the wall thickness is overestimated, and the radius of curvature is underestimated, inducing an important underestimation of regional systolic wall stress. This 3-D approach easily used with 3-D MR technique may be the method of choice for calculating regional wall stress in patients with ventricular deformations.

The significant correlation between the end-systolic wall stress and the EF and volumes may provide evidence that an alteration of the systolic performance is

largely due to an increase in regional wall stress. Development of a compensatory eccentric ventricular hypertrophy normally leads to normalization of the wall stress of the healthy zones (3). In our study, this compensatory hypertrophy was observed in inferior infarction and was associated with no increase of the wall stresses in the healthy zone. However, the normal wall stress found is probably due more to a lack of cavity dilatation, as observed in our patients. Conversely, in anterior infarction where end-diastolic and end-systolic volumes of the left ventricle are increased and associated with a decrease of EF, the wall stresses remain abnormal in the healthy zone, without important compensatory left ventricular hypertrophy. Therefore, most of the changes in wall stress in the noninfarcted regions are due to cavity dilatation, not to changes in wall thickness, as reported by others (15, 18, 24). It can be speculated in patients with anterior infarct that the rate of hypertrophy no longer keeps pace with the rate of dilation. Consequently, the wall thickness does not increase or even gets thinner as dilation progresses, and the wall stress increases rapidly, causing a decrease in EF.

Echocardiography is a simple and widely available examination, but it relies on geometric assumptions. However, the assessment of the left ventricular geometry in patients with infarction is complex and needs a tridimensional approach without any geometric assumptions allowed only by MRI. Moreover, the wall stress estimations by echocardiography are usually provided at the level of papillary muscle insertions or at the level of the tips of mitral valve leaflets, as opposed to MRI, which permits a local measurement of the wall stress.

Study limitations. An invasive measurement or an indirect calculation of the peak systolic blood pressure only provides a global value for the whole ventricle. Consequently, the regional variations of the wall stress are induced by those of the geometric factor but do not integrate the local changes in pressure. The reliability of the wall stress measurement depends on the limitation of patient movements between two breath holds. The effect of the axial twist on the determination of the wall stress between two adjacent sections was minimized by averaging the local wall stresses determined for 16 sectors. The true apex and base were not covered in the assessment of regional wall stress which makes measurements primarily in the mild left ventricle. Two others limitations should be mentioned: the absence of age-matched control group and the wide standard deviation of the mean time to imaging.

In conclusion, this study shows that MRI allows quantification of the regional variations of wall stress and that a tridimensional approach is better than the others two methods for precise evaluation of the regional wall stress. In patients with inferior infarction, the increase in wall stress remains localized in the infarcted region. In patients with anterior infarction, the increase of wall stress is diffuse but predominates at the level of the infarcted region, despite a successful reperfusion of the artery involved and administration

of an inhibitor of the angiotensin-converting enzyme and a β -blocker. This increase in wall stress could be an important prognostic factor of left ventricular remodeling.

REFERENCES

- Balzer P, Furber A, Cavaro-Ménard C, Croué A, Tadéi A, Geslin P, Jallet P, and Le Jeune JJ. Simultaneous and correlated detection of endocardial and epicardial borders on short-axis cardiac MR images for the measurement of left ventricular mass. *Radiographics* 18: 1009–1018, 1998.
- Balzer P, Furber A, Delépine S, Rouleau F, Lethimonier F, Morel O, Tadéi A, Jallet P, Geslin P, and Le Jeune JJ. Regional assessment of wall curvature and wall stress in the left ventricle with magnetic resonance imaging. *Am J Physiol Heart Circ Physiol* 277: H901–H910, 1999.
- Beltrami CA, Finato N, Rocco M, Feruglio GA, Puricelli C, Cigola E, Quaini F, Sonnenblick EH, Olivetti G, and Anversa P. Structural basis of end-stage failure in ischemic cardiomyopathy in humans. *Circulation* 89: 151–163, 1994.
- Beyar R, Shapiro EP, Graves WL, Rogers WJ, Guier WH, Carey GA, Soulen RL, Zerhouni EA, Weisfeldt ML, and Weiss JL. Quantification and validation of left ventricular wall thickening by a three-dimensional volume element magnetic resonance imaging approach. *Circulation* 81: 297–307, 1990.
- Burton AC. The importance of the shape and size of the heart. *Am Heart J* 54: 801–810, 1957.
- Doughty RN, Whalley GA, MacMahon S, and Sharpe N. Left ventricular remodeling with carvedilol in patients with congestive heart failure due to ischemic heart disease. *J Am Coll Cardiol* 29: 1060–1066, 1997.
- Fleagle SD, Thedens DR, Ehrhardt JC, Scholtz TD, and Skorton DJ. Automated identification of left ventricular borders from spin-echo magnetic resonance images. *Invest Radiol* 26: 295–303, 1991.
- Furber A, Balzer P, Cavaro-Ménard C, Croué A, Da Costa E, Lethimonier F, Geslin P, Tadéi A, Jallet P, and Le Jeune JJ. Experimental validation of an automated edge detection method for a simultaneous determination of the endocardial and epicardial borders in short-axis cardiac MR images: application in normal volunteers. *J Magn Reson Imaging* 8: 1006–1014, 1998.
- Ginzton LE, Rodrigues D, Shapiro SM, Laks MM, Conant R, and Lobodzinski SM. Estimation of regional end-systolic wall stress during exercise in coronary artery disease. *Am Heart J* 13: 733–746, 1966.
- Grossman W, Braunwald E, Mann T, McLaurin L, and Green L. Contractile state of the left ventricle in man as evaluated from end-systolic pressure-volume relations. *Circulation* 56: 845–852, 1977.
- Hutchins GM and Bukley BH. Infarct expansion versus extension: two different complications of acute myocardial infarction. *Am J Cardiol* 41: 1127–1132, 1978.
- Janz R. Estimation of local myocardial stress. *Am J Physiol Heart Circ Physiol* 242: H875–H881, 1982.
- Jeremy RW, Hackworthy RA, Bautovich G, Hutton BF, and Harris PJ. Infarct artery perfusion and change in left ventricular volume in the month after acute myocardial infarction. *J Am Coll Cardiol* 19: 989–995, 1987.
- Kittleson MD, Knowlen GG, and Johnson LE. Early and late global and regional left ventricular function after experimental transmural myocardial infarction: relationships of regional wall motion, wall thickening, and global performance. *Am Heart J* 114: 70–78, 1987.
- Kramer CM, Lima JAC, Reichek N, Ferrari VA, Llaneras MR, Palmon LC, Yeh IT, Tallant B, and Axel L. Regional differences in function within noninfarcted myocardium during left ventricular remodeling. *Circulation* 88: 1279–1288, 1993.
- Lessick J, Sideman S, Azhari H, Shapiro EP, Weiss JL, and Beyar R. Evaluation of regional load in acute ischemia by three-dimensional curvatures analysis of the left ventricle. *Ann Biomed Eng* 21: 147–161, 1993.
- McKay RG, Pfeffer MA, Pasternak RC, Markis JE, Come PC, Nakao S, Alderman JD, Ferguson JJ, Safian RD, and Grossman W. Left ventricular remodeling after myocardial infarction: a corollary to infarct expansion. *Circulation* 74: 693–702, 1986.
- Mitchell GF, Lamas GA, Vaughan DE, and Pfeffer MA. Left ventricular remodeling in the year after first anterior myocardial infarction: a quantitative analysis of contractile segment lengths and ventricular shape. *J Am Coll Cardiol* 19: 1136–1144, 1992.
- Pfeffer MA, Lamas GA, Vaughan DE, Parisi AF, and Braunwald E. Effect of captopril on progressive ventricular dilatation after anterior myocardial infarction. *N Engl J Med* 319: 80–86, 1988.
- Pouleur H, Rousseau MF, Van Eyll C, and Charlier AA. Assessment of regional left ventricular relaxation in patients with coronary artery disease: importance of geometric factors and change in wall thickness. *Circulation* 69: 696–702, 1984.
- Pouleur H, Rousseau MF, Van Eyll C, Van Mechelen H, Brasseur LA, and Charlier AA. Assessment of left ventricular contractility from late systolic stress-volume relations. *Circulation* 65: 1204–1212, 1982.
- Pouleur HG, Konstam MA, Udelson JE, and Rousseau MF. Changes in ventricular volume, wall thickness and wall stress during progression of left ventricular dysfunction. The SOLVD Investigators. *J Am Coll Cardiol* 22, Suppl A: 43A–48A, 1993.
- Reichek N. Noninvasive determination of left ventricular end-systolic stress: validation of the method and initial application. *Circulation* 65: 98–108, 1982.
- Rumberger JA, Behrenbeck T, Breen JR, Reed JE, and Gersh BJ. Nonparallel changes in global left ventricular chamber volume and muscle mass during the first year after transmural myocardial infarction in humans. *J Am Coll Cardiol* 21: 673–682, 1993.
- Segar DS, Moran M, and Ryan T. End-systolic regional wall stress-length and stress-shortening relations in an experimental model of normal, ischemic and reperfused myocardium. *J Am Coll Cardiol* 17: 1651–1660, 1991.
- Solomon SD, Aikawa Y, and Martini MS. Assessment of regional left ventricular wall stress after myocardial infarction by echocardiography-based structural analysis. *J Am Soc Echocardiogr* 11: 938–947, 1998.
- Van der Geest RJ and Reiber JHC. *Quantification of Global and Regional Left Ventricular Function by MRI*. Amsterdam: Kluwer, 1998, p. 233–246.
- Van Gilst WH, Kingma JH, Peels KH, Dembrink JE, and St. John Sutton M. Which patients benefit from early angiotensin-converting enzyme inhibition after myocardial infarction? Results of one-year serial echocardiographic follow-up from the captopril and thrombolysis study (CATS). *J Am Coll Cardiol* 28: 114–121, 1996.
- White HD, Norris RM, Brown MA, Brandt PWT, Whitlock RML, and Wild CJ. Left ventricular end-systolic volume as the major determinant of survival after recovery from myocardial infarction. *Circulation* 76: 44–51, 1987.
- Zhang J, Wilke N, Wang Y, Zhang Y, Wang C, Eijgelshoven MHJ, Cho YK, Murakami Y, Ugurbil K, Bache RJ, and From AHL. Functional and bioenergetic consequences of postinfarction left ventricular remodeling in a new porcine model. *Circulation* 94: 1089–1100, 1996.